GAMMA SPECTROSCOPY OF NEUTRON-DEFICIENT NUCLEI CLOSE TO ^{70}Br USING THE EAGLE ARRAY AND ANCILLARY DETECTORS AT THE HEAVY ION LABORATORY IN WARSAW*

D. Duda [a], M. Matejska-Minda [a], A. Fijałkowska [b], G. Jaworski [c], I. Kuti [d], A. Malinowski [b,c], M. Palacz [c], P. Sekrecka[c], G. de Angelis[e], P. Bednarczyk [a], T. Cap [f], M. Ciemała [a], N. Cieplicka-Oryńczak [a], G. Colucci [c], I. Dedes [a], J.M. Deltoro[g,h], N. Erduran[i], K. Gajewska [a], A. Goasduff [e], V. González[h], J. Grębosz [a], K. Hadyńska-Klęk [c], Ł. Iskra [a], P. Kulessa[a], M. Kmiecik[a], M. Komorowska[c], M. Kopeć[b], M. Kowalczyk[c], J.A. Kowalska[c], A. Krakó[d,j], B. Kruzsicz[d,j], M. Loriggiola[e], M. Matuszewski[c], K. Mazurek [a], J. Molnár[d], P.J. Napiorkowski [c], A. Otręba[b], M. Pęgier[c], W. Poklepa[b], M. Regulska[b], J. Samorajczyk-Pyśk[c], E. Sanchis[h], O. Stezowski[k], A. Stolarz[c], A. Špaček[c], N. Toniolo[e], J. Towers[l], K. Wrzosek-Lipska[c]

[a]Institute of Nuclear Physics Polish Academy of Sciences, Kraków, Poland
[b]Faculty of Physics, University of Warsaw, Warszawa, Poland
[c]Heavy Ion Laboratory, University of Warsaw, Warszawa, Poland
[d]HUN-REN Institute for Nuclear Research, Debrecen, Hungary
[e]INFN, Laboratori Nazionali di Legnaro, Legnaro, Italy
[f]National Centre for Nuclear Research, Świerk, Poland
[g]Instituto de Física Corpuscular, CSIC-Universidad de Valencia, Valencia, Spain
[h]Department of Electronic Engineering, University of Valencia, Valencia, Spain
[i]Faculty of Engineering and Natural Sciences
Istanbul Sabahattin Zaim University, Istanbul, Turkey
[j]University of Debrecen, Doctoral School of Physics, Debrecen, Hungary
[k]Universite Claude Bernard Lyon 1, CNRS/IN2P3, IP2I Lyon, France
[l]Department of Physics, University of York, York, UK

Received 19 December 2025, accepted 19 January 2026, published online 31 March 2026

The $A = 70$, $T = 1$ isobaric multiplet exhibits an anomalous Coulomb energy difference (CED) behavior, with the ^{70}Br/^{70}Se pair showing a decrease in CED with increasing spin, contrary to the typical trend observed

* Presented at the XXXVIII Mazurian Lakes Conference on Physics, Piaski, Poland, August 31–September 6, 2025.

in other pf-shell nuclei. To investigate this phenomenon, a dedicated experiment was carried out at the Heavy Ion Laboratory of the University of Warsaw using an 88 MeV ^{32}S beam impinging on a ^{40}Ca target. Excited states in $A \approx 70$ neutron-deficient nuclides were populated in fusion–evaporation reactions. Gamma rays were measured with the EAGLE spectrometer, whereas the reaction channel identification was provided by the combined set of neutron — NEDA and charged particle — DIAMANT detectors. Preliminary data analysis shows the satisfactory performance of the setup, which will allow for in-depth studies of the structure of the nuclei of interest.

DOI:10.5506/APhysPolBSupp.19.1-A20

1. Introduction

The structure of nuclei lying along the $N = Z$ line in the $A \approx 70$ mass region has attracted considerable interest. In these systems, protons and neutrons may occupy the same orbitals, leading to enhanced proton–neutron (pn) correlations that compete with like-nucleon pairing [1]. Different particle configurations can drive these nuclei towards spherical, prolate, oblate, triaxial, or even octupole-deformed shapes [2]. Shell-model and mean-field studies predict rapid configuration changes along the $N = Z$ line that affect macroscopic observables such as the moment of inertia; a pronounced variation is expected around $N = Z = 35$ (^{70}Br) [3].

Total energy surface calculations for the neighboring $N = Z$ nuclei ^{68}Se and ^{72}Kr show a characteristic shape coexistence pattern (prolate in ^{68}Se; oblate/triaxial minima in ^{72}Kr) [4–6]. Experimental lifetime studies in this region indicate moderate elongation with significant triaxiality and possible shape instability with increasing rotational frequency [7]. Nuclei near $N = Z$ provide a sensitive testing ground for isospin symmetry and its breaking through the Coulomb interaction. The Coulomb energy difference (CED) between $T = 1$ analog states is a powerful structural probe, sensitive to deformation, nuclear radii, and alignment effects with spin [8–10]. While CED values in the pf shell typically increase with spin, the ^{70}Br/^{70}Se pair exhibits an anomalous decrease, suggesting an unusual structural evolution. In ^{70}Se, an oblate ground state and unstable prolate deformation at low spin ($J^\pi < 8^+$) have been reported [11, 12], and high-spin studies suggest an increase of prolate deformation above the crossing [13]. Mirror-nucleus data point to a larger deformation in ^{70}Kr than in ^{70}Se [14].

Previous spectroscopy of ^{70}Br using the ^{40}Ca(^{32}S, pn) and ^{40}Ca(^{36}Ar, $\alpha\, pn$) reactions established parts of the level scheme but reported weak (and partly inconsistent) $6^+ \to 4^+$ (963 keV) and $8^+ \to 6^+$ (1025 keV) transitions

[15–17]. The present HIL115 experiment was designed to revisit the high-spin structure of ^{70}Br and clarify the CED evolution with spin using clean channel selection.

2. Experimental setup and data analysis

The experiment was performed at the Heavy Ion Laboratory (HIL), University of Warsaw, in December 2023, employing the EAGLE–NEDA–DIAMANT setup [18–20]. An attempt to populate excited states in ^{70}Br was carried out via the fusion–evaporation reaction ^{40}Ca(^{32}S, pn)^{70}Br. A ^{32}S beam of 88 MeV, delivered by the U-200P cyclotron, was chosen to maximize the yield of the (pn) channel according to GEMINI++ estimates. The typical beam intensity was ∼1 pnA over a 14-day data-taking period.

The target consisted of 0.8 mg/cm^2 enriched ^{40}Ca evaporated onto a 12 mg/cm^2 Au backing and protected by a 100 μg/cm^2 Au layer to prevent oxidation [21]. Furthermore, the target was mounted under oxygen-free conditions in an argon-filled chamber to minimize the risk of oxidation. Gamma rays were detected with the EAGLE spectrometer comprising 15 Compton-suppressed HPGe detectors. To identify reaction channels, EAGLE was coupled to two ancillary systems: NEDA and DIAMANT (72 CsI(Tl)).

The experimental data from the NEEDLE (EAGLE+NEDA) [22] and DIAMANT detector systems [23] were merged using the OFEVENT framework, which combines the independent data into a single, time-correlated event structure using NEDA timing signal as a reference. This procedure ensures a consistent synchronization of γ-ray, neutron, and charged-particle

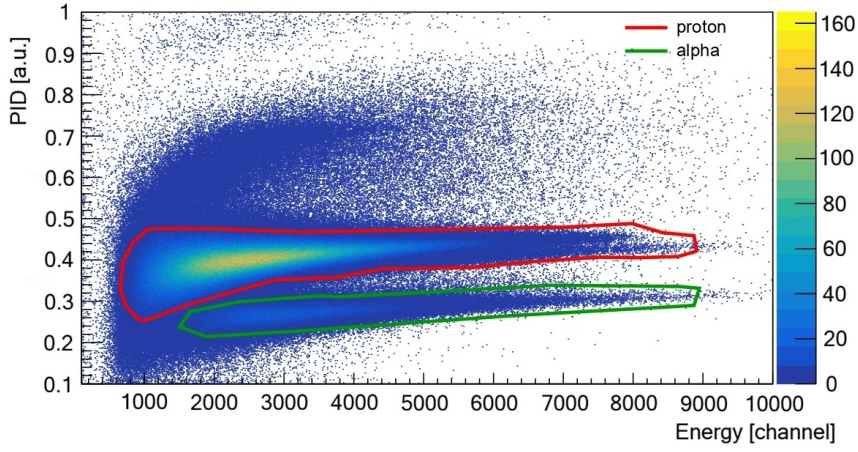

Fig. 1. PID (particle identification parameter) graph as a function of energy for a single DIAMANT element. The contours corresponding to protons and α particles illustrate the gates used to select the reaction channel.

information for subsequent analysis. The energy calibration and control of the stability was done separately. The gating procedure on the DIAMANT detector is shown in Fig. 1

3. Results

To obtain an overview of all products populated in the ^{32}S+^{40}Ca fusion–evaporation reaction, a total projection spectrum was first generated by showing all γ-ray events without any gating conditions. The lower panel of Fig. 2 shows the resulting spectrum. Numerous transitions originating from nuclei produced on the target assembly and contamination as oxygen and carbon are visible. Strong lines associated with ^{42}Ca, ^{69}As, ^{66}Ge, ^{46}Ti, and Coulomb excitation of ^{197}Au can be identified. This inclusive spectrum illustrates the complexity of the reaction environment and provides an important reference for assigning γ transitions to specific evaporation residues.

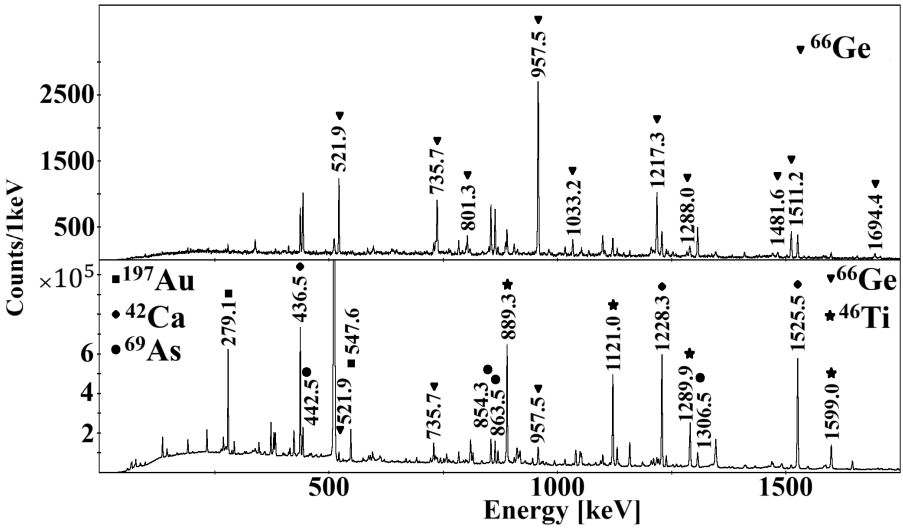

Fig. 2. Upper panel: γ-ray spectrum gated on the $\alpha 2p$ condition in DIAMANT, showing transitions assigned to ^{66}Ge. Lower panel: total projection spectrum without particle gating, revealing γ-ray contributions from several reaction products populated in the reaction of the ^{32}S beam on ^{40}Ca but also on ^{16}O and ^{12}C contaminations.

To enhance selectivity toward specific channels, particle-coincidence conditions were applied using the DIAMANT detector. The upper panel of Fig. 2 shows the spectrum obtained with the $\alpha 2p$ gate. Under this condition, transitions attributed to ^{66}Ge dominate the spectrum, in accordance with the expected population of the ($\alpha 2p$) evaporation channel. There are also weak contributions from other products populated in the reaction. The

clear identification of known ^{66}Ge transitions confirms the correct performance of the particle-identification scheme and the ability of DIAMANT to isolate different reaction channels containing charged particles.

To illustrate the selectivity of the setup, a two-dimensional γ–γ coincidence matrix was constructed. Summing of multiple coincidence gates significantly reduces background and enhances transitions correlated with specific channels. A summed coincidence spectrum was generated by gating on transitions corresponding to the ^{69}As in coincidence with the $3p$ condition in DIAMANT. The resulting spectrum is presented in Fig. 3. This $3p$ gate strongly enhances γ rays associated with the ^{69}As evaporation residue. Several intense transitions characteristic of ^{69}As are clearly visible, together with numerous weaker lines corresponding to higher-lying states. The most prominent peaks match well the known γ-ray energies reported in earlier studies, confirming the presence and clean identification of ^{69}As in the present data. The overall peak-to-background conditions demonstrate good coincidence quality and validate the robustness of the particle-identification procedure used for channel selection.

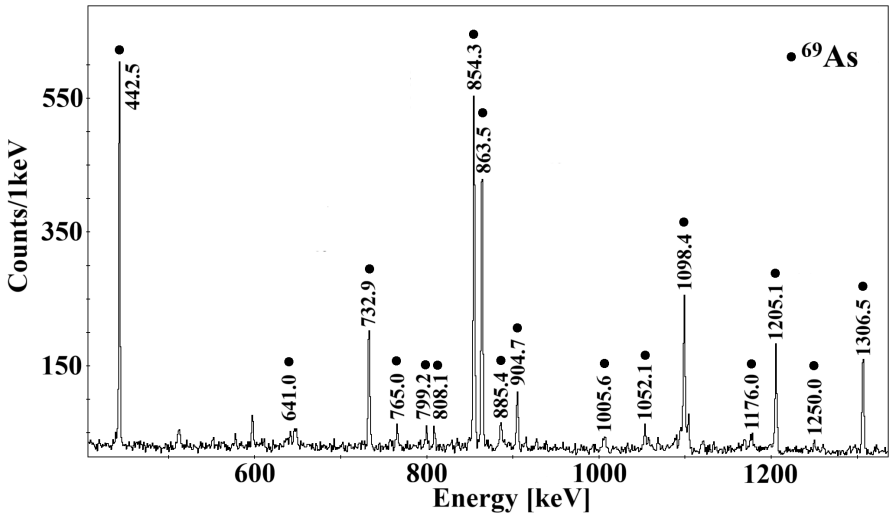

Fig. 3. Summed γ–γ coincidence spectrum, gated by the $3p$ condition in DIAMANT and obtained by setting gates on the strongest γ-ray transitions of ^{69}As (the 442, 732, 854, 863, 904, 1098, 1205, and 1306 keV lines). All γ-ray lines of ^{69}As visible in the spectrum are indicated in the figure.

The successful identification of ^{69}As in the respective gates confirms the effectiveness of the particle-identification scheme and the overall quality of the present data. The gold backing thickness was optimized to stop evaporation residues. In the further analysis, reaction channels selected by charged-

particle conditions will be examined in detail, including the application of Doppler correction procedures. This will significantly improve the resolution for fast-moving evaporation residues and is expected to facilitate the identification of γ-ray transitions from higher-lying, short-lived states.

This work is supported by the National Science Centre (NCN), Poland, under the SONATA BIS-13 grant agreement No. 2023/50/E/ST2/00621. The installation and use of NEDA at HIL were supported by the NCN grants No. 2020/39/D/ST2/00466 and 2023/51/D/ST2/02816. This project has received funding from the European Union's Horizon Europe Research and Innovation programme under grant agreement No. 101057511 (EURO-LABS). The European Gamma-Ray Spectroscopy Pool (GAMMAPOOL) is acknowledged for providing HPGe detectors.

REFERENCES

[1] W. Nazarewicz *et al.*, *Nucl. Phys. A* **435**, 397 (1985).
[2] A.V. Afanasjev, S. Frauendorf, *Phys. Rev. C* **71**, 064318 (2005).
[3] M. Hasegawa *et al.*, *Phys. Lett. B* **656**, 51 (2007).
[4] A. Gaamouci *et al.*, *Phys. Rev. C* **103**, 054311 (2021).
[5] E. Bouchez *et al.*, *Phys. Rev. Lett.* **90**, 082502 (2003).
[6] E. Clément *et al.*, *Phys. Rev. C* **75**, 054313 (2007).
[7] M. Matejska-Minda *et al.*, *Phys. Rev. C* **100**, 054330 (2019).
[8] C.D. O'Leary *et al.*, *Phys. Lett. B* **525**, 49 (2002).
[9] M.A. Bentley, S.M. Lenzi, *Prog. Part. Nucl. Phys.* **59**, 497 (2007).
[10] B.S. Nara Singh *et al.*, *Phys. Rev. C* **75**, 061301 (2007).
[11] J. Ljungvall *et al.*, *Phys. Rev. Lett.* **100**, 102502 (2008).
[12] J. Heese *et al.*, *Z. Phys. A* **325**, 325 (1986).
[13] G. Rainovski *et al.*, *J. Phys. G: Nucl. Part. Phys.* **28**, 2617 (2002).
[14] K. Wimmer *et al.*, *Phys. Rev. Lett.* **126**, 072501 (2021).
[15] G. de Angelis *et al.*, *Eur. Phys. J. A* **12**, 51 (2001).
[16] D.G. Jenkins *et al.*, *Phys. Rev. C* **65**, 064307 (2002).
[17] D.M. Debenham *et al.*, *Phys. Rev. C* **94**, 054311 (2016).
[18] J. Mierzejewski *et al.*, *Nucl. Instrum. Methods Phys. Res. A* **659**, 84 (2011).
[19] J. Valiente-Dobón *et al.*, *Nucl. Instrum. Methods Phys. Res. A* **927**, 81 (2019).
[20] J.N. Scheurer *et al.*, *Nucl. Instrum. Methods Phys. Res. A* **385**, 501 (1997).
[21] M. Matejska-Minda *et al.*, HIL University of Warsaw, Annual Report, 2023.
[22] G. Jaworski *et al.*, *Acta Phys. Pol. B Proc. Suppl.* **17**, 3-A12 (2024).
[23] I. Kuti *et al.*, *Acta Phys. Pol. B Proc. Suppl.* **17**, 3-A13 (2024).